International Journal of Fluid Power 3 (2002) No.2 pp. 47-54

ESTABLISHING OPERATING POINTS FOR A LINEARIZED MODEL OF A LOAD SENSING SYSTEM

Duqiang Wu, Richard Burton, Greg Schoenau and Doug Bitner

Department of Mechanical Engineering, University of Saskatchewan
57 Campus Drive, Saskatoon, Saskatchewan, Canada, S7N 5A9
duw612@mail.usask.ca

Abstract

A load sensing system is one in which the pump flow is adjusted to keep pressure across an orifice constant and independent of any variation in the load pressure. This ensures that the pressure losses across the orifice are kept to a minimum which increases efficiency substantially. Because the system is closed loop, stability can become a problem. To establish stability bounds, linearized analysis is often employed. However, to do this, operating points of all linearized parameters and coefficients must be established as a function of certain parameters such as load pressure. This can only be done by solving a series of nonlinear algebraic equations. This paper presents a set of equations for three special conditions. The experimental verification of operating points that are predicted for such a load sensing system is presented. The three regions are established theoretically and are verified experimentally. It is found that the operating points undergo a noticeable change when in transition from one region to another (as dictated by variations in load pressure or orifice area). It was also found that the agreement between the predicted and measured operating points was quite satisfactory and could be used with confidence in future studies.

Keywords: load sensing, steady state operating point, transition point, pressure regulator, pressure control pump

1 Introduction

Small signal analysis, in which nonlinear behavior is linearized about an operating point, has been used for many years. The power of this approach has been utilized to its fullest extent in classical fluid power text books such as Merrit (1967), a book used by fluid power designers and students alike. Despite the advent of sophisticated simulation packages that can handle nonlinear describing equations, the development of linearized models is still one of the most effective tools in assisting designers and students in understanding how dynamic systems and components interact and how stability can be affected by changing certain parameters. However, to use linearized models effectively, knowledge of all the operating points for different loading conditions must be known. In many cases, values of some linearized coefficients are approximated by assuming typical operating points for loading conditions. However, parameters or coefficients which must be evaluated at operating points are not independent of each other and must be solved for simultaneously. Because of the complexity of some models, solving for these parameters and coefficients is a difficult process.

The system under consideration in this paper is a load sensing pump. This is a system that utilizes interaction between many components to function properly. These components are a load, flow control orifice, load sensing spool, control piston and variable displacement pump (pressure control pump). A typical load sensing configuration that is commonly found in industrial applications is shown in Fig. 1. The objective of the load sensing pump and regulator is to maintain a constant pressure drop across an orifice. If the area of the orifice is fixed, then flow control results. The controller element that tries to maintain the pressure drop across the orifice is called pressure regulator (Fig. 1). The actual pressure drop across the orifice is fed back to this compensator and compared to a desired pressure drop. If the required pressure differential is not accomplished, then an imbalance across the spool occurs and a displacement results. This shift in spool displacement results in fluid being ported to or from the control piston via the pump pressure line or to tank return line. The subsequent movement in the control piston either increases or decreases the pump displacement (flow) to establish the desired pressure differential across the orifice.

This manuscript was received on 11 February 2002 and was accepted after revision for publication on 8 July 2002

This particular system (and variations thereof) has been studied extensively using both linearized and non-linear approaches. Of particular interest in this paper are the works of Bitner (1984), Palmberg (1985), Lin (1988), Krus (1988), Zhang (1989), Ding (1989), Lantto (1990, 1991), Pettersson (1996), Elfving (1997) and Erkkilä (1999), in which linearized models were used for analysis and design. Bitner (1984) considered the measurement techniques necessary to determine LS pump parameters. It was found that two factors, fluid temperature and the operating point, greatly affected the flow gain and flow-pressure sensitivity of the orifice, pump leakage, and frequency response. He developed a simplified model based on a transfer function analysis applied to a linearized model. The correlation between the experimental and theoretical results was poor. Part of the problem was the choice of the operating point for the frequency response. This study was one of the first to report this problem. Although Bitner (and others) discovered that the operating point greatly affected the theoretical results, no attempt was made to assess the effect of operating point selection. Most researchers who have used linearization and transfer function analysis have not adequately dealt with this "crucial" problem.

A recent study initiated by Wu (2002) considered the load sensing pump in Fig. 1 and introduced the steady state describing equations necessary to define the steady state operating conditions of the load sensing system. These equations were manipulated to represent three unique operating conditions of the system. By solving the steady state nonlinear algebraic equations which resulted from linearization, values for operating parameters could be solved. Using three possible positions of the load sensing spool under steady state conditions, three unique operating conditions were defined from which critical parameter values were ascertained for each of these regions. The critical parameters were related to the design and "adjustable" or "pre-set" parameters of the hydraulic components. Wu's paper did present some preliminary experimental results (swash plate angle as a function of load pressure and valve orifice area). This paper will substantially expand both the experimental procedures that were used to obtain the operating conditions of the load sensing system and the solutions of the model. Pump pressure, control spool chamber pressure, pressure regulator spool displacement, pressure differential across the orifice and swash plate angle are measured experimentally and compared to their theoretical counterparts. Discussion on differences and physical interpretations of the results are presented.

2 Modelling of the Load Sensing System

Consider the load sensing model shown in Fig. 1. A model of this system has been developed and presented by Wu (2002) and will not be repeated here. A pressure regulator with a critically lapped spool has three steady state conditions (defined as Conditions I, II, and III) as shown in Fig. 2. Under steady state conditions, the net flow rate into the control chamber should be zero because the control pressure and the swash plate angle are constant.

For Condition I: $x_{r0} = 0$ ($Q_{r1} = 0$ and $Q_{r2} = 0$); this condition is obvious because the valve is critically lapped.

For condition II: $x_{r0} > 0$ ($Q_{r1} = 0$); this only occurs if $P_{s0} = P_{y0}$.

For condition III: $x_{r0} < 0$ ($Q_{r2} = 0$); this can only occur if $P_{y0} = 0$and $P_T = 0$.

In the system shown in Fig. 1, the load pressure is a variable which is dependant upon the load parameters. To demonstrate the existence of the three operating conditions and verify the analysis, the load pressure is kept constant.

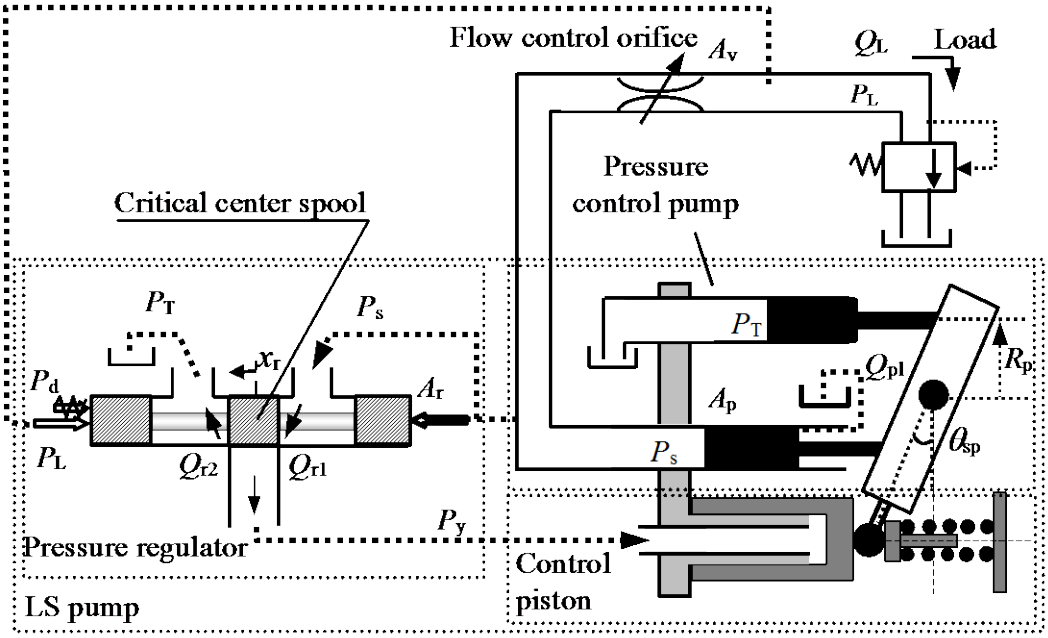

Fig. 1: *Schematic of the load sensing pressure compensating system*

No loss of generality occurs because a controlled load pressure, P_{L0}, now an input, is all that is needed to simulate a steady state load condition. Experimentally, a pressure relief whose characteristics were well known created this load.

The steady state equations in Wu (2002) were solved simultaneously to yield the operating points associated with the required parameters. Depending on the compensator spool location (see Fig. 2), three unique operating conditions must be considered.

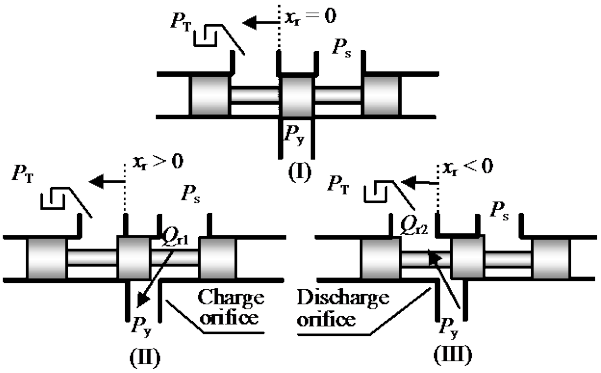

Fig. 2: *Three operation conditions of LS spool (I) critically lapped (II) control chamber charged (III) the control chamber discharged*

Condition I

Under the critically lapped condition, the pressure differential across the flow control valve is equal to the constant, P_d, due to x_{r0} being zero. The pump pressure, P_{so}, the swash plate angle, θ_{sp0}, and the control pressure, P_{yo}, can be derived to be:

$$P_{s0} = P_d + P_{L0} \tag{1}$$

$$\theta_{sp0} = \tan^{-1}\left[\frac{\pi\left(C_d A_v\sqrt{\frac{2}{\rho}P_d} + c_{pl}\left(P_d + P_{L0}\right)\right)}{NA_p R_p \omega}\right] \tag{2}$$

$$\begin{aligned} P_{y0} &= T_{sp} + K_{pr2}\left(P_d + P_{L0}\right) \\ &\quad -\left(K_{sp} + K_{pr3}\left(P_d + P_{L0}\right)\right)\theta_{sp0} \end{aligned} \tag{3}$$

P_y consists of equivalent pressures due to the pretension in the spring, the spring extension and the force of the pump pistons on the swash plate.

Condition II

For condition II P_{so} can be found by numerically solving the nonlinear equation (note, all other parameters and coefficients are known):

$$\begin{aligned} &\frac{NA_p R_p \omega}{\pi}\tan\left(\frac{T_{sp} + \left(K_{pr2} - 1\right)P_s}{K_{sp} + K_{pr3}P_s}\right) \\ &\quad - c_{pl}P_s - C_d A_v\sqrt{\frac{2}{\rho}\left(P_s - P_{L0}\right)} = 0 \end{aligned} \tag{4}$$

Eq. 4 is valid only if the pump pressure satisfies condition II (i.e., $x_{r0} > 0$ or $P_{s0} - P_{L0} > P_d$). Since $P_{s0} = P_{y0}$, the swash plate angle can be determined by

$$\theta_{sp0} = \frac{T_{sp} + \left(K_{pr2} - 1\right)P_s}{K_{sp} + K_{pr3}P_s} \tag{5}$$

Condition III

Condition III represents the case where the control pressure, P_{y0}, is zero and the pump is fully stroked. Therefore, the swash plate angle is the maximum, θ_{spmax}. Under the assumption that the leakage of the pump is negligible compared to the load flow through the valve, P_{so} can be solved from the equation:

$$P_{s0} = P_{L0} + \frac{\rho}{2}\left(\frac{NA_p R_p \omega \tan\theta_{spmax}}{\pi C_d A_v}\right)^2 \tag{6}$$

For condition III (i.e., $P_{s0} - P_{L0} < P_d$ or $P_{s0} < P_d + P_{L0}$), the orifice area of the flow control valve, A_v, must satisfy the condition:

$$A_v > \frac{NA_p R_p \omega \tan\theta_{spmax}}{\pi C_d\sqrt{\frac{2}{\rho}P_d}} \tag{7}$$

Given these three conditions, the challenge was to devise a system and test procedure that could create each of the three conditions experimentally and to verify the theoretical prediction of the value of the operating points of selected parameters as a function of load pressure and control valve area (considered inputs in this study).

3 Experimental Test System and Procedures

The experimental system illustrated in Fig. 1 was used to verify the steady state operating conditions as a function of load pressure and control valve area. A load sensing pump (Vickers PVE19Q) was used in this study. The load sensing regulator on this pump was modified to provide an accurate measurement of the spool position. This was critical to the study because an accurate position of the spool with respect to the control chamber (Fig. 1) was required to accurately define the three operating regions (Fig. 2) and the transition from one region to the other. The flow control orifice was created by a needle valve (manufactured by Deltrol Corp) and, as has been mentioned, the load was simulated by a two-stage relief valve (Vickers CT06F50). Pump and valve parameters for the simulation were obtained from direct measurements or from previous studies (Kavanagh, 1987; Bitner, 1984). A summary of the measured parameter values is given in Table 1. Parameters A_r and k_r in Table 1 were used to determine the system differential pressure, P_d (Wu, 2002).

Table 1: Parameters of the LS pump

ω	1800	rpm
A_p	2.07×10^{-4}	m^2
N	9	
R_p	3.48×10^{-2}	m
A_r	3.17×10^{-5}	m^2
k_r	6.11×10^{4}	N/m
T_{sp}	1.11×10^{6}	N/m^2
K_{sp}	1.42×10^{6}	
K_{pr2}	0.28	N/m^2 rad
K_{pr3}	0.45	rad^{-1}
θ_{spmax}	0.314	rad

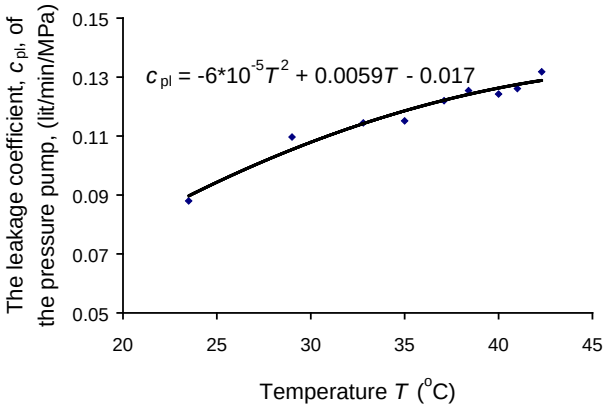

Fig. 3: *Leakage coefficient of LS pump*

In addition to these parameters, the leakage coefficient of the pump, c_{pl}, and the discharge coefficient of the needle valve, C_d, were required. As discussed in Wu (2002), the leakage coefficient was dependent on the fluid temperature. The experimental leakage coefficient as a function of temperature is shown in Fig. 3. In Wu (2002), the discharge coefficient, C_d, was evaluated as a function of fluid temperature, pressure drop and orifice opening (expressed as a number of valve turns). For 2.5 turns, the expression for the discharge coefficient obtained from a statistical curve fit to the experimental data is

$$C_d(T, \Delta P)\big|_{2.5\text{turns}} = 6.35\times10^{-4}T^2 + 5.39\times10^{-2}T - 1.59\times10^{-2}\Delta P^2 + 0.231\Delta P - 3.78\times10^{-3}T\Delta P - 0.511 \quad (8)$$

The measurement system and DAQ system consisted of three pressure sensors, an angular position sensor (RVDT), a spool position sensor (proximity probe), a thermocouple and a multifunction interface board. This instrumentation was used to measure six variables; the pump pressure, P_s, the control pressure, P_y, the load pressure, P_L, the swash plate angle, θ_{sp}, the load sensing spool displacement, x_r, and the fluid temperature, T. The fluid temperature was used to determine the discharge coefficient and to ensure that repeatability of results could be established.

In order to obtain the complete signals using the DAQ system, a high sampling frequency (5000 Hz) was used. It was observed that most of the signal outputs contained significant components at frequencies of 270 Hz and 540 Hz introduced by the axial piston variable displacement pump. In practice, the sampling frequency should be five to ten times the maximum significant signal frequency to ensure the signal is correctly reproduced. All the data collected from the DAQ system was further processed by filtering out all of the dynamic components with a 3rd order Butterworth filter to obtain the SSOP of the LS system.

In order to force the pump to operate in the three steady state conditions and the transition regions (conditions I and II, and conditions I and III), the system parameter, P_d, and the controlled inputs, A_v and P_{L0} had to be carefully chosen. Two sets of experiments were designed to do this. In the first set, the pump operated in conditions I and II and its transition region. To do this, P_d was set to 0.58 MPa by adjusting the initial position of the LS spool to – 0.3 mm, Fig. 2 (III) and the needle valve was opened 2.75 turns (i.e., cross sectional area of 10 mm^2). The load pressure was slowly increased (so that system transients would not be excited) with a ramp input signal (e.g. 0.2 MPa/s) to a proportional relief valve and the steady state relationships were deduced at many points along the trace.

The second set of experiments was used to force the pump to operate in conditions I and III. In this set of experiments, the needle valve took on a range of settings while the relief valve setting was held constant (but P_L did not stay constant). Twenty different points of the needle valve opening were tested so that the SSOP could be plotted with respect to the variation in valve opening (or, the corresponding sectional area of the valve orifice). This set of experiments was further repeated five times to present the statistical results of the SSOP of the LS system. It was observed that there is scatter at specific points of valve opening. This was attributed partly to the visual error of setting the same valve opening at different tests.

4 Comparison of the Experimental and Theoretical Results

As discussed above, the steady state operating conditions were examined under the three conditions specified. The operating points at various load pressures and valve areas were of interest over the full expected operating ranges but the transition from condition I to II and conditions I and III were also important. It should be noted that the transition from condition II to condition III is not physically possible since $x_{r0} = 0$ lies in between these conditions.

Conditions I and II

$x_{r0} = 0$ ($Q_{r1} = 0$ and $Q_{r2} = 0$) and $x_{r0} > 0$ ($Q_{r1} = 0$)

Figure 4 through 7 show comparisons of the theoretical and experimental results with a valve opening of 2.75 turns. Figure 4 shows the steady state operating point for P_{s0} and P_{y0} as a function of P_{L0}. If the load pressure is less than 0.8 MPa (116 psi), the theoretical calculation indicates that the LS system operates under

condition II and the pump pressure, P_{s0}, approaches the control pressure, $P_{y0.}$ The agreement between the theoretical prediction and the measured values for the control pressure is very good over all load pressures but is poor for the pump pressure as the operating point approaches the transition region. This is understandable because the measured P_{s0} will always be larger than P_{y0} under all circumstances due to leakage from the control chamber. Leakage was not included in the model. Thus, $P_{s0,}$ theoretically, is underestimated and will have an affect in under-estimating other parameters. This is apparent in subsequent figures in which P_{s0} is a factor.

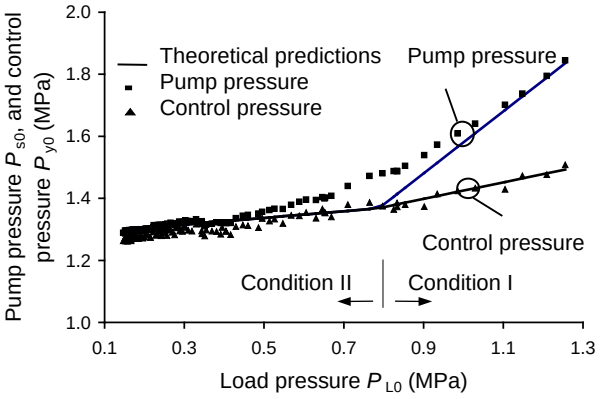

Fig. 4: *System pressures (condition I and II)*

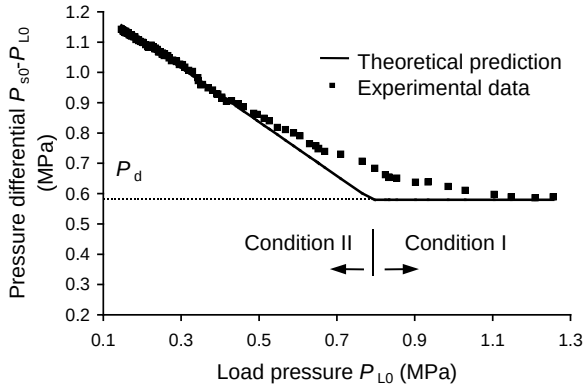

Fig. 5: *Pressure differential (condition I and II)*

Figure 5 shows the measurement of the system pressure differential, P_{s0}–P_{L0} as a function of P_{L0}. Under condition II, the experimental pressure differential is larger than the theoretical value. This is a reasonable result given that the theoretical P_{s0} consistently predicts a lower value in the transition region. When the system operating condition moves from condition II to I, the pressure differential approaches a constant value that, in fact, is P_d.

Figure 6 shows that the predicted and theoretical LS spool displacements are non-zero which is a necessary condition for the existence of condition II. The trends in the experimental and theoretical results are similar. Since spool displacements are inherently a function of P_{s0}, then errors in the theoretical values of P_{s0} will be reflected indirectly in the prediction of the spool displacements.

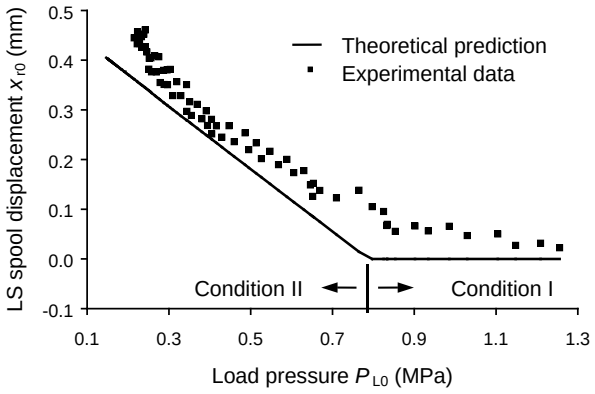

Fig. 6: *LS spool position (condition I and II)*

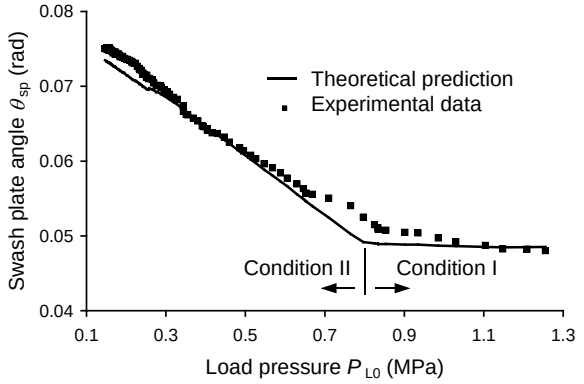

Fig. 7: *Swash plate angle (condition I and II)*

Figure 7 shows the swash plate angle as a function of P_{L0}. The agreement between the predicted and measured operating points is quite acceptable for most of the region. The consequence of errors in the predicted P_{s0} are less significant. It is observed that the both the predicted and measured swash plate angle decrease as the load pressure increases in P_{L0} (condition II). This has a physical explanation. In condition II, the flow through the valve orifice decreases as the pressure differential (P_{s0}–P_{L0}) decreases (note: the orifice opening is fixed). This can be true only if the swash plate angle decreases. In condition I, although the pump leakage increases slightly as P_{s0} increases due to the load pressure increase, P_{L0}, the load flow decreases as the pressure differential (P_{s0}–P_{L0}), continuously decreases. The overall flow delivered by the pump pistons decreases as the load pressure increases. This can also be true only if the swash plate angle decreases (albeit, small).

It is also observed in Fig. 4 through 7 that the theoretical calculation yields a distinct boundary between conditions II and I, This is not observed in the experimental results in which a smooth transition from condition I to condition II prevails. This is because a practical LS hydraulic system is very complex which no theoretical model can exactly represent. The theoretical model was derived from several assumptions: the leakage through the clearance between the load sensing spool land and the sleeve was neglected, and the nonlinearity of the load sensing spring and coulomb fric-

tion of the load sensing spool were neglected. Finally, small chamfers at the edge of the needle valve orifice were not considered in the model. The presence of these factors in a physical system tends to smooth discontinuities which can exist in theoretical models. Regardless, the results are considered to be sufficient for linearized analysis that require steady state operating point parameter predictions.

Condition I and III

(Q_{r1}= 0 and Q_{r2} = 0) and $x_{r0} < 0$ (Q_{r2} = 0)

Condition III will occur if the opening of the flow control valve increases beyond a certain value. Therefore, the condition III operating points use the valve opening, A_v, to be the controlled variable and hence, the independent variable. This is different from the study for conditions I and II in which the opening of the valve was fixed and the load pressure varied independently. In the experimental testing, the load pressure was not varied using the relief valve as before; it was set at 1.5 MPa. However, in reality, given the pressure flow characteristics of the relief valve (known), the load pressure was not constant but a function of flow which occurred as a result of changes in the opening of the needle valve (sectional area of the valve orifice). When the system reached condition III in which the swash plate was fully stroked, then the flow through the relief valve became constant and hence P_{Lo} became constant. This is shown in Fig. 8.

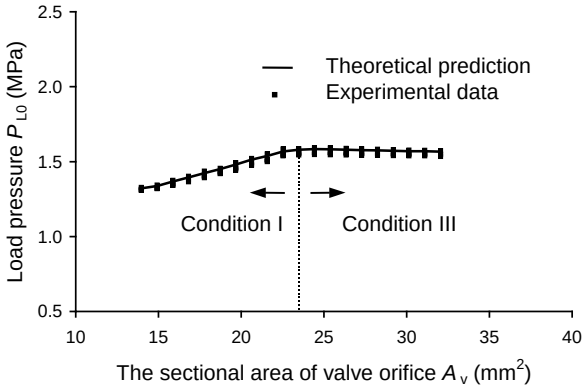

Fig. 8: *Load pressure (condition I and III)*

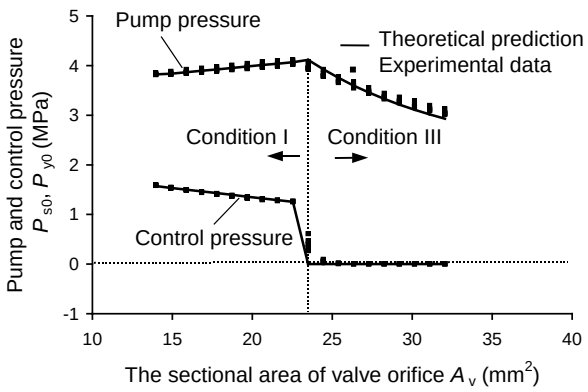

Fig. 9: *System pressures (condition I and III)*

Figure 9 shows the pump pressure, P_{s0}, and the control pressure, P_{y0}, as a function of the opening of the valve. It is evident that the LS system makes a sudden transition from condition I to condition III both experimentally and theoretically. The control pressure, P_y, suddenly drops to zero. This occurs because, at the transition point, the pump is fully stroked. Subsequent increases in the orifice area do not change the load pressure (fully stroked, constant flow) but do decrease the pump pressure. The pressure drop across the compensator spool displaces the spool to the $x_v < 0$ region and the control port is now completely vented to tank.

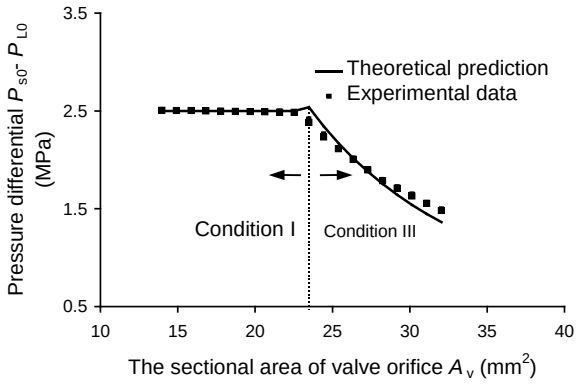

Fig. 10: *Pressure differential (condition I and III)*

Figure 10 shows the pressure differential, P_{s0}–P_{L0}, as a function of A_v. In condition I, the pressure differential, P_{s0}–P_{L0}, is controlled to the design value, P_d, which is 2.5 MPa. When the system passes through condition III, the pressure differential decreases due to the constant load flow (pump stroked) and the increasing opening of the needle valve. As discussed above, a decrease of the pressure differential causes the LS spool to move into the $x_{r0} < 0$ region. Since P_{y0} is equal to zero, the pressure differential simply follows changes in P_{so}.

Figure 11 and 12 illustrate the changes in the swash plate angle and the spool displacement as a function of the valve orifice areas. The results are consistent with physical reasoning as has been alluded to in the above discussions. In Fig. 9 though 11, the agreement between the predicted and measured results is quite exceptional. Even the predicted transition discontinuities are in agreement. However, Fig. 12 shows that there are some significant differences between the theoretical and experimental results. Even though the trends of the measurement and theoretical predictions are same, an offset of 0.1 mm exists. Leakage across the load sensing spool could have caused this. Fig. 7 also indicates that the theory underestimates the measured spool displacement results. In the experimental system, spool land leakage would cause the pressure P_{s0} at the side of proximity probe to become smaller which would result in an increase in the actual spool displacement. Another possible reason for the offset could be a consequence of a null position error, which could be introduced by visually identifying the null position during the calibration of the proximity measurement system. At this point, these factors have not been substantiated.

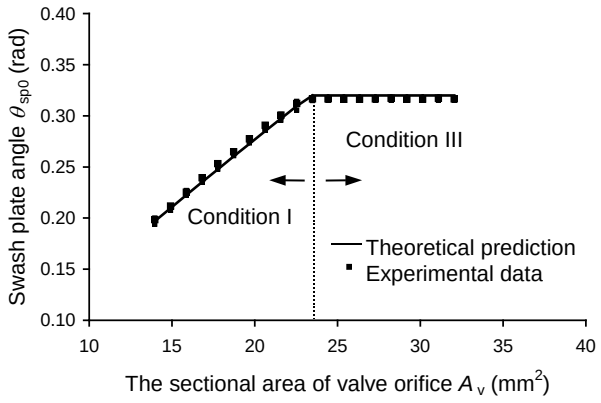

Fig. 11: *Swash plate angle (condition I and III)*

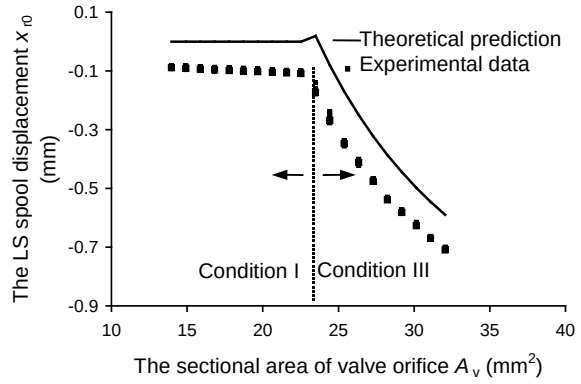

Fig. 12: *LS spool position (condition I and III)*

5 Conclusions

Knowledge of the steady state operating conditions of a load sensing pump system must be well established before conducting a dynamic analysis. Because the pressure regulator spools are critically lapped, models of the load sensing system become piecewise nonlinear which results in three different steady state models for different operating conditions. In this paper, the three conditions were investigated experimentally and compared to their theoretical counterparts developed by Wu (2002). The experiments indicated that the three conditions predicted theoretically do exist in the load sensing system studied. For each condition, the experimental results show an acceptable repeatability. The experiments also show a smooth transition between the three conditions, which is different from the theoretical predictions. Condition I is the "normal" operating condition. Conditions II and III should be avoided.

This paper also suggests how parameters/variables determine operating conditions. The steady state operating conditions of the load sensing system depend on the system pressure differential setting, P_d, the load pressure, P_{L0}, and the opening of the flow control valve, A_v. When both P_d and P_{L0} are small, condition II occurs. When the demand flow is larger than the flow supplied by the load sensing pump (i.e., the opening of the valve, A_v, is larger than some critical value), condition III occurs.

In short, this research verifies the existence of three operating conditions and gives the method of justifying the operating conditions and the equations of calculating the steady state operating points. This work is now being extended to include the operating points in a dynamic model of the system. These operating points can be used to establish realistic conditions for stable operation. The approach is also being extended to include a pressure compensated flow control valve in a load sensing system.

Nomenclature

"$_0$"	subscript "0" represents SSOP
A_p	sectional area of pump pistons
A_r	sectional area of LS spool
A_v	sectional area of valve's orifice
C_d	discharge coefficient of orifice
c_{pl}	pump leakage coefficient
k_r	LS spool spring constant
K_{pr2}	Pressure torque constant
K_{pr3}	Pressure torque constant
K_{sp}	Angular effective spring coefficient
N	the number of pump pistons
P_d	setting of valve pressure drop
P_L	load pressure
P_s	pump pressure
P_T	tank pressure
P_y	control pressure
Q_{pl}	pump leakage
Q_{r1}	flow of charge orifice of control chamber
Q_{r2}	flow of discharge orifice of control chamber
R_p	distance of pump pistons axis from the pump shaft
T	fluid temperature
T_{sp}	Angular effective spring pretension
x_r	LS spool displacement
θ_{sp}	swash plate angle
ρ	fluid density
ω	pump shaft speed

References

Bitner, D. and **Burton, R. T.** 1984. Experimental Measurement of Load Sensing Pump Parameters. *Proceedings of the 40th National Conference on Fluid Power*, Chicago, p. 153.

Bitner, D. and **Burton, R. T.** 1984. Small Signal Model of a Load Sensing Pump. *Proceedings of the 40th National Conference on Fluid Power*, Chicago, p. 107.

Ding, K. 1989. The Simplification of Transfer Function with Literal Coefficients in Hydraulic System. *Proceedings of the 2nd International Conference on Fluid Power Transmission and Control*, Hangzhou, China, p. 409.

Elfving, M., Palmberg, J.-O. and **Jansson, A.** 1997. Distributed Control of Fluid Power Actuators - a Load Sensing Application of a Cylinder with Decoupled Chamber Pressure Control. *Proceedings of the 5th Scandinavian International Conference on Fluid Power, SICFP'97*, Linkoping, Sweden, p. 159.

Erkkila, M. 1999. Practical Modelling of Load-Sensing Systems. *Proceeding of the 6th Scandinavian International Conference on Fluid Power, SICFP'99*, Tampere, Finland, p. 445.

Kavanagh, G. P. 1987. *The Dynamic Modeling of an Axial Piston Hydraulic Pump*. M.Sc. thesis, University of Saskatchewan, Canada.

Krus, P. 1988. *On Load Sensing Fluid Power Systems*. Dissertation No. 198, Linkoping University, Sweden.

Lantto, B., Palmberg, J. O. and **Krus, P.** 1990. Static and Dynamic Performance of Mobile Load-sensing Systems with Two Different Types of Pressure-Compensated Valves. *SAE Technical Paper Series, SAE*, Sept 10-13, p. 251.

Lantto, B., Krus, P. and **Palmberg, J. O.** 1991. Interaction between Loads in Load-sensing Systems. *Proceedings of the 2nd Tampere International Conference on Fluid Power*, Linköping, Sweden, p. 53.

Lin, S. J. and **Akers, A.** 1988. The Control of an Axial Piston Pump: Use of a Two-stage Electrohydraulic Servovalve. *Proceedings of the 43rd National Conference on Fluid Power*, Chicago, p. 443.

Merritt, H. E. 1967. *Hydraulic control systems.* John Wiley & Sons, Inc.

Palmberg, J. O., Krus, P. and **Ding, K.** 1985. Dynamic Response Characteristics of Pressure-Control Pumps. *The 1st International Conference on Fluid Power Transmission and Control*, Zhejiang University, Hangzhou, China, p. 110.

Pettersson, H., Krus, P., Jansson, A. and **Palmberg, J. O.** 1996. The Design of Pressure Compensators for Load Sensing Hydraulic Systems. *UKACC International Conference on Control'96*, IEE 427. University of Exeter, UK, p. 1456.

Zhang, Z. and **Hou, S.** 1989. Experiment and Research of Model XBPOC-F75FF Pressure-flow Compensated Load-sensing Axial Piston Pump. *Proceedings of the 2nd International Conference on Fluid Power Transmission and Control*, Zhejiang University, Hangzhou, China, p. 317.

Zarotti, L. G. and **Nervegna, N.** 1988. Saturation Problems in Load Sensing Architectures. *Proceedings of the 43rd National Conference on Fluid Power, NCFP*, Chicago, p. 393.

Wu, D. 2002. Steady State Analysis of the Load Sensing Systems. *Proceedings of the 2nd FPNI PhD Symposium 2002*, Modena, Italy.

Duqiang Wu
Graduate student for Ph.D. at present, Mechanical Engineering Department, University of Saskatchewan in Canada. Master (1984) at Nanjing University of science and Technology in China. Engineer (1986) at Shaanxi Mechanical and Electrical Institute in China. Visiting Scholar (1997) at University of Illinois at Urbana-Champaign.

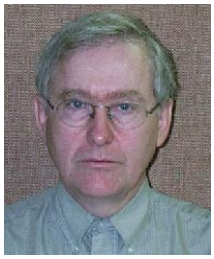

Richard Burton
P.Eng, Ph.D, Assistant Professor Mechanical Engineering, Professor, Mechanical Engineering, University of Saskatchewan. Burton is involved in research pertaining to the application of intelligent theories to control and monitoring of hydraulics systems, component design, and system analysis. He is a member of the executive of ASME, FPST Division, a member of the hydraulics' advisory board of SAE and NCFP and a convenor for FPNI.

Greg Schoenau
Professor of Mechanical Engineering at the University of Saskatchewan. He was head of that Department from 1993 to 1999. He obtained B.Sc. and M. Sc. Degrees from the University of Saskatchewan in mechanical engineering in 1967 and 1969, respectively. In 1974 he obtained his Ph.D. from the University of New Hampshire in fluid power control systems. He continues to be active in research in this area and in the thermal systems area as well. He has also held positions in numerous outside engineering and technical organizations.

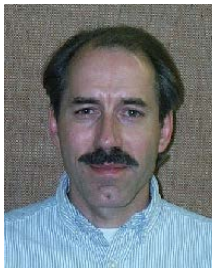

Doug Bitner
MSc. Departmental Assistant Mechanical Engineering, University of Saskatchewan.
Manager Fluid Power Laboratory and Control Systems Laboratory University of Saskatchewan.